

Supplementary material:

Enhancing electrochemical capacitor performance of N-doped tannin-derived carbons by hydrothermal treatment in ammonia

Oscar Pinto-Burgos^{a,b*}, Jimena Castro-Gutiérrez^c, Po Shan Poon^b, Maria T. Izquierdo^d, Alain Celzard^{c,e}, Vanessa Fierro^{c,**} Juan Matos^{f,**}

^a Departamento de Ingeniería Química, Facultad de Ingeniería, Universidad de Concepción, Barrio Universitario s/n, Chile.

^b Unidad de Desarrollo Tecnológico, UDT, Universidad de Concepción, Barrio Universitario s/n, Concepción, Chile.

^c Université de Lorraine, CNRS, IJL, F-88000, Epinal, France.

^d Instituto de Carboquímica (ICB-CSIQ), Miguel Luesma Castán 4, E-50018, Zaragoza, Spain.

^e Institut Universitaire de France (IUF), 75005 Paris, France.

^f Unidad de Cambio Climático y Medio Ambiente (UCCMA), Instituto Iberoamericano de Desarrollo Sostenible (IIDS), Facultad de Arquitectura, Construcción y Medio Ambiente, Universidad Autónoma de Chile, Temuco 4780000, Chile.

* Corresponding Author

** Corresponding Authors

E-mails addresses: oscpinto@udec.cl (O. Pinto-Burgos); juan.matos@uautonoma.cl (J. Matos); Vanessa.Fierro@univ-lorraine.fr (V. Fierro).

Phones: +56 9 78064083, +56 9 9379 8340, +33 (0)372 749 677

Keywords: Tannin; Capacitance; Nitrogen doping; Carbon materials; Sustainable energy.

Trassatti's method

In Trassatti's method, the charge (q) in the voltammetry test is assumed to depend on the scan rate (v) as follows:

$$q = q_{\infty} + a_1 v^{-1/2} \quad (\text{S1})$$

$$\frac{1}{q} = \frac{1}{q_T} + a_2 v^{1/2} \quad (\text{S2})$$

where a_1 and a_2 are constants, q_{∞} is the charge not limited by ion diffusion ($v \rightarrow \infty$), and q_T is the total cell charge ($v \rightarrow 0$). If the measurements are carried out under the same conditions, they can be applied in terms of capacitance as follows:

$$C_{(v)} = a_1 v^{-1/2} + C_{EDL} \quad (\text{S3})$$

$$\frac{1}{C_{(v)}} = a_2 v^{1/2} + \frac{1}{C_T} \quad (\text{S4})$$

where C_{EDL} is the capacitance arising from the electric double-layer (not limited by ion diffusion) and C_T is assumed to be the total capacitance, such as:

$$C_T = C_{PSC} + C_{EDL} \quad (\text{S5})$$

where C_{PSC} is the capacitance arising from Faradaic contributions.

Figure S5C) and S5D) show, as an example, the intercept values of the linear regression for sample N8THC900-2 for equations S3 and S4, respectively.

Supplementary tables

Table S1. Summary of burn-off (BO), elemental analysis and XPS quantification.

Carbons	BO (%)	Elemental analysis				XPS		
		C (wt.%)	H (wt.%)	N (wt.%)	O (wt.%)	C (at.%)	N (at.%)	O (at.%)
THC800	0 ^a	94.5	0.8	0.2	4.5	97.3	N.D.	2.7
THC800-1	10.0	93.6	0.8	0.2	5.4	97.4	N.D.	2.6
THC800-2	14.9	93.3	0.7	0.2	5.8	97.2	N.D.	2.8
THC800-4	24.9	92.8	0.8	0.2	6.2	97.8	N.D.	2.2
N4THC800	0 ^a	87.4	1.3	4.6	6.7	93.6	3.6	2.8
N4THC800-1	10.6	87.3	1.3	3.6	7.8	94.8	3.0	2.2
N4THC800-2	18.1	87.5	1.2	3.4	7.9	94.7	3.0	2.3
N4THC800-4	42.9	82.2	1.4	3.2	13.2	93.0	3.3	3.7
N4THC900-1	35.3	87.8	1.3	3.7	7.2	94.5	3.1	2.4
N4THC900-1.5	49.8	88.1	1.5	3.5	6.9	94.7	2.6	2.6
N4THC900-2	70.0	86.7	1.5	3.0	8.8	94.3	2.8	2.9
N8THC800	0 ^a	87.5	1.5	4.8	6.2	92.6	3.9	3.5
N8THC800-1	10.2	88.0	1.4	4.2	6.4	93.9	2.8	3.3
N8THC800-2	16.4	88.1	1.4	4.2	6.3	92.7	4	3.3
N8THC800-4	27.8	81.8	1.6	3.5	13.1	92.8	3.9	3.3
N8THC900-1	21.2	87.6	1.5	3.5	7.4	94.1	2.7	3.2
N8THC900-1.5	50.2	87.4	1.4	3.5	7.7	94.0	3.1	2.9
N8THC900-2	59.9	87.3	1.4	3.3	8.0	93.5	3.9	2.6

^a These zero burn-off values correspond to non-activated samples. However, mass losses on pyrolysis (800 °C, 1h) were not zero, being equal to approximately 60%, 48%, and 47% 60 %, 48 %, and 47 % for TCH800, N4TCH800 and N8TCH800, respectively. The remaining values correspond to a true burn-off, i.e., are the mass losses obtained after activation with CO₂.

Table S2. Relative atomic composition (at. %) of deconvoluted C 1s peaks for tannins-derived carbons and N-doped tannins-derived nanoporous carbons.

Carbon sample	C 1s ^a						
	C _D 283.5	C _{sp²} 284.4	C ₂ 285.5	C ₃ 286.4	C ₄ 287.6	C ₅ 289.2	C _{π-π*} 291
THC800	0.0	64.2	25.5	0.0	0.8	6.3	3.2
THC800-1	0.0	66.3	25.1	0.0	0.7	5.7	2.3
THC800-2	0.0	67.4	24.1	0.0	0.9	5.4	2.3
THC800-4	0.0	67.1	23.8	0.0	0.8	5.4	2.9
N4THC800	5	55.1	19.7	11.5	3.6	3.1	1.9
N4THC800-1	8.2	56.9	15.2	12.1	2.1	3.5	2.1
N4THC800-2	3.9	55	16.6	15.8	2.6	3.9	2.2
N4THC800-4	5.5	56.5	15.5	13.7	3.4	2.9	2.5
N4THC900-1	1.5	60.6	16.5	12	3	3.6	2.8
N4THC900-1.5	0.7	61.1	18.1	9.4	4.1	3.6	3
N4THC900-2	1.2	58.3	15.6	12.2	4.2	4.3	4.3
N8THC800	2.4	54.5	17.7	13.1	5	3.9	3.3
N8THC800-1	2.7	57.3	17.8	10.6	4.7	3.7	3.2
N8THC800-2	2.8	56.6	20	10.3	4.4	3.4	2.5
N8THC800-4	4.3	62.9	15.5	10.8	2.8	2.7	1.1
N8THC900-1	2.4	60.5	16.4	10.6	3.5	3.8	2.9
N8THC900-1.5	2.7	61.2	15.2	11.1	3.3	3.7	2.8
N8THC900-2	2.1	57	17.1	11.2	4.7	4.2	3.7

^a C_D: carbon associated with defects like in five-atom rings and/or graphitic carbon nitrides; C_{sp²}: graphitic carbon; C₂: carbon with sp³ hybridization; C₃: ether- or hydroxyl-bonded C, or C bonded to nitrogen oxides; C₄: carbon in lactones or pyridones; C₅: carboxylic acids; C_{π-π*}: HUMO-LUMO transitions associated with the C_{sp²} peak.

Table S3. Relative atomic composition (at. %) of deconvoluted O 1s and N 1s peaks for tannins-derived carbons and N-doped tannins-derived nanoporous carbons.

Carbon sample	O 1s ^a					N 1s ^b			
	O1	O2	O3	O=N	H ₂ O	N6	N5	NQ	N=O
	530.9	532.3	533.1	534.1	534.9	398.3	400.2	401.2	402.9
THC800	26.6	0.0	66.0	N.D.	7.4	N.D.	N.D.	N.D.	N.D.
THC800-1	37.9	0.0	49.6	N.D.	12.5	N.D.	N.D.	N.D.	N.D.
THC800-2	30.3	0.0	58.7	N.D.	11.0	N.D.	N.D.	N.D.	N.D.
THC800-4	37.0	0.0	56.2	N.D.	6.8	N.D.	N.D.	N.D.	N.D.
N4THC800	59.2	21.2	12.4	3.9	3.3	31.3	24.2	33.6	11.0
N4THC800-1	63.4	16.9	13.5	2.3	3.9	29.5	23.1	31.9	15.4
N4THC800-2	58.6	17.7	16.8	2.8	4.2	32.9	28.2	29.4	9.4
N4THC800-4	61.4	16.8	14.9	3.7	3.2	35.2	19.5	34.3	11.0
N4THC900-1	63.3	17.2	12.5	3.1	3.8	34.0	24.7	30.8	10.5
N4THC900-1.5	63.4	18.8	9.8	4.3	3.7	33.6	29.3	25.7	11.3
N4THC900-2	61.6	16.5	12.9	4.4	4.5	34.6	20.2	32.4	12.7
N8THC800	57.9	18.8	13.9	5.3	4.1	32.9	30.3	27.6	9.2
N8THC800-1	60.9	18.9	11.3	5.0	3.9	30.8	25.2	31.5	12.6
N8THC800-2	59.8	21.1	10.9	4.6	3.6	31.3	27.1	30.6	11.0
N8THC800-4	66.4	16.4	11.4	3.0	2.9	32.6	24.0	30.1	13.2
N8THC900-1	63.8	17.3	11.2	3.7	4.0	28.9	25.0	31.2	14.9
N8THC900-1.5	64.8	16.1	11.7	3.5	3.9	33.5	25.1	31.0	10.3
N8THC900-2	60.5	18.2	11.9	5.0	4.5	37.3	25.6	25.7	11.3

^a **O1**: C=O double bonds such as quinone-type groups; **O2**: aliphatic C-O such as bonds in phenols and ether groups; **O3**: aromatic C-O such as in carboxylic acids; **O=N**: oxygen bound to nitrogen.

^b **N6**: pyridinic groups; **N5**: pyrrolic or pyridonic groups; **NQ**: graphitic carbon nitrides; **N=O**: nitrogen bound to oxygen.

Table S4. Textural properties obtained from N₂ and H₂ adsorption isotherms at -196 °C.

Carbons	A_{BET} (m ² g ⁻¹)	SSA (m ² g ⁻¹)	$V_{0.97}$ (cm ³ g ⁻¹)	V_{T} (cm ³ g ⁻¹)	$\langle w_{\text{u}\mu} \rangle$ (nm)	$V_{\text{u}\mu}$ (cm ³ g ⁻¹)	$\langle w_{\text{s}\mu} \rangle$ nm	$V_{\text{s}\mu}$ (cm ³ g ⁻¹)	$\langle w_{\text{meso}} \rangle$ (nm)	V_{meso} (cm ³ g ⁻¹)
THC800	505	990	0.173	0.339	0.5	0.182	1.0	0.065	21.7	0.091
THC800-1	655	1100	0.214	0.380	0.5	0.203	1.0	0.084	19.0	0.093
THC800-2	680	1110	0.229	0.421	0.5	0.206	1.0	0.089	22.8	0.126
THC800-4	730	1150	0.304	0.570	0.5	0.206	1.0	0.104	25.0	0.260
N4THC800	450	905	0.378	0.848	0.5	0.170	1.1	0.043	28.5	0.636
N4THC800-1	620	1020	0.403	0.854	0.5	0.172	1.0	0.090	27.0	0.592
N4THC800-2	675	1090	0.420	0.866	0.5	0.180	1.0	0.100	25.7	0.586
N4THC800-4	905	1200	0.519	1.080	0.5	0.178	1.1	0.178	26.4	0.727
N4THC900-1	1000	1350	0.597	1.170	0.5	0.194	1.0	0.191	26.5	0.789
N4THC900-1.5	1210	1490	0.701	1.360	0.5	0.194	1.0	0.265	25.9	0.901
N4THC900-2	1415	1710	0.908	1.670	0.5	0.173	1.1	0.362	24.6	1.186
N8THC800	420	910	0.175	0.385	0.5	0.175	1.1	0.044	24.2	0.166
N8THC800-1	560	995	0.228	0.474	0.5	0.174	1.0	0.078	27.3	0.223
N8THC800-2	630	1080	0.268	0.589	0.5	0.196	1.0	0.083	28.3	0.310
N8THC800-4	805	1180	0.316	0.613	0.5	0.216	1.1	0.125	27.0	0.272
N8THC900-1	830	1230	0.339	0.611	0.5	0.186	1.0	0.148	19.1	0.277
N8THC900-1.5	1410	1610	0.553	0.970	0.5	0.196	1.1	0.353	23.4	0.422
N8THC900-2	1645	1720	0.641	1.080	0.5	0.180	1.1	0.447	21.2	0.449

A_{BET} : Area estimated through the BET method; SSA: surface area estimated from PSDs obtained by applying the 2D-NLDFT-HS kernel; $V_{0.97}$: Gurvich volume; V_{T} : total volume estimated from the PSDs obtained by applying the 2D-NLDFT-HS kernel; $\langle w_{\text{u}\mu} \rangle$: average ultramicropores size; $V_{\text{u}\mu}$: ultramicropore volume; $\langle w_{\text{s}\mu} \rangle$: average supermicropores size; $V_{\text{s}\mu}$: supermicropore volume; $\langle w_{\text{meso}} \rangle$: average mesopore size; V_{meso} : mesopore volume.

Supplementary figures

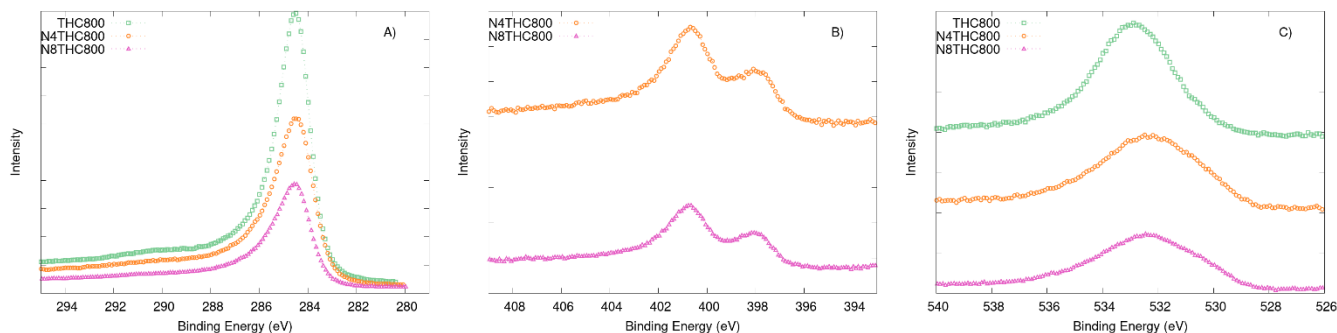


Figure S1. XPS spectra of: A) C 1s; B) N 1s; and C) O 1s regions for THC800, N4THC800 and N8THC800 samples.

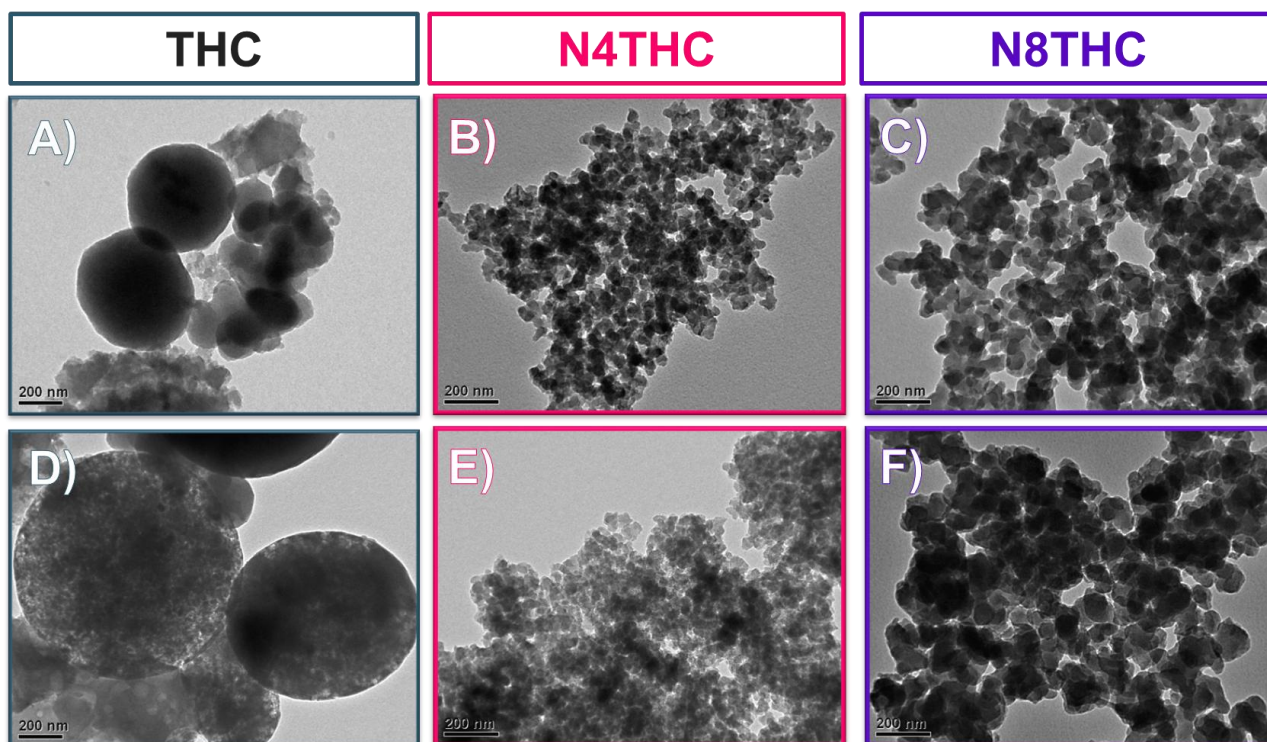


Figure S2. TEM images for: A-C) materials obtained by hydrothermal carbonization, coded from left to right as THC, N4THC, and N8THC, and D-F) respective materials carbonized at 800 °C, coded from left to right as THC800, N4THC800, and N8THC800.

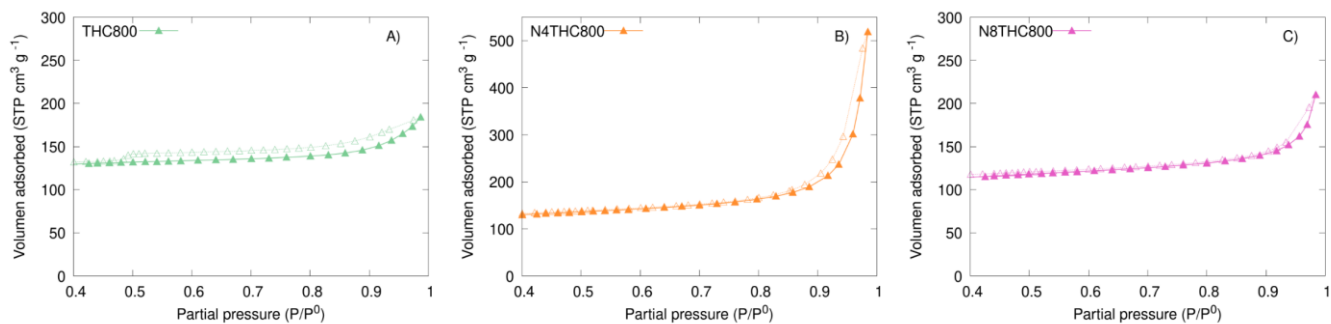


Figure S3. N₂ adsorption (solid symbols) – desorption (empty symbols) isotherms at -196 °C of non-activated samples: A) THC800; B) N4THC800; and C) N8THC800.

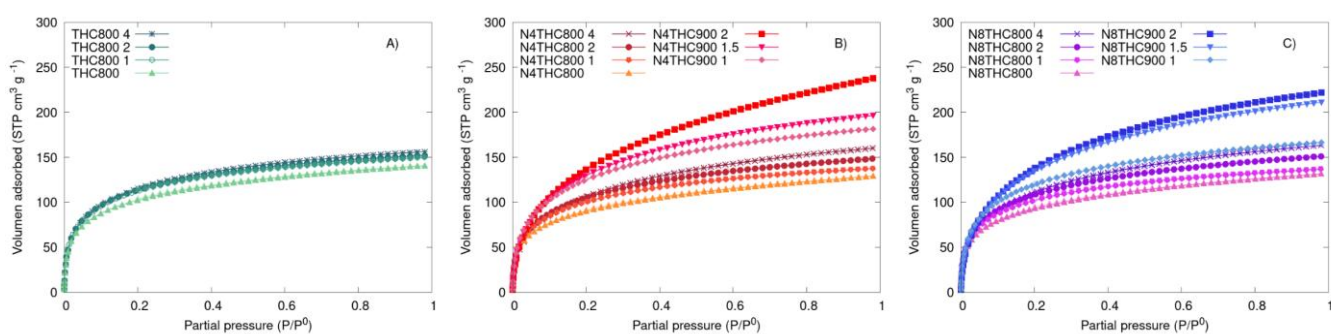


Figure S4. H₂ adsorption isotherms at -196 °C for: A) THC series; B) N4THC series; and C) N8THC series.

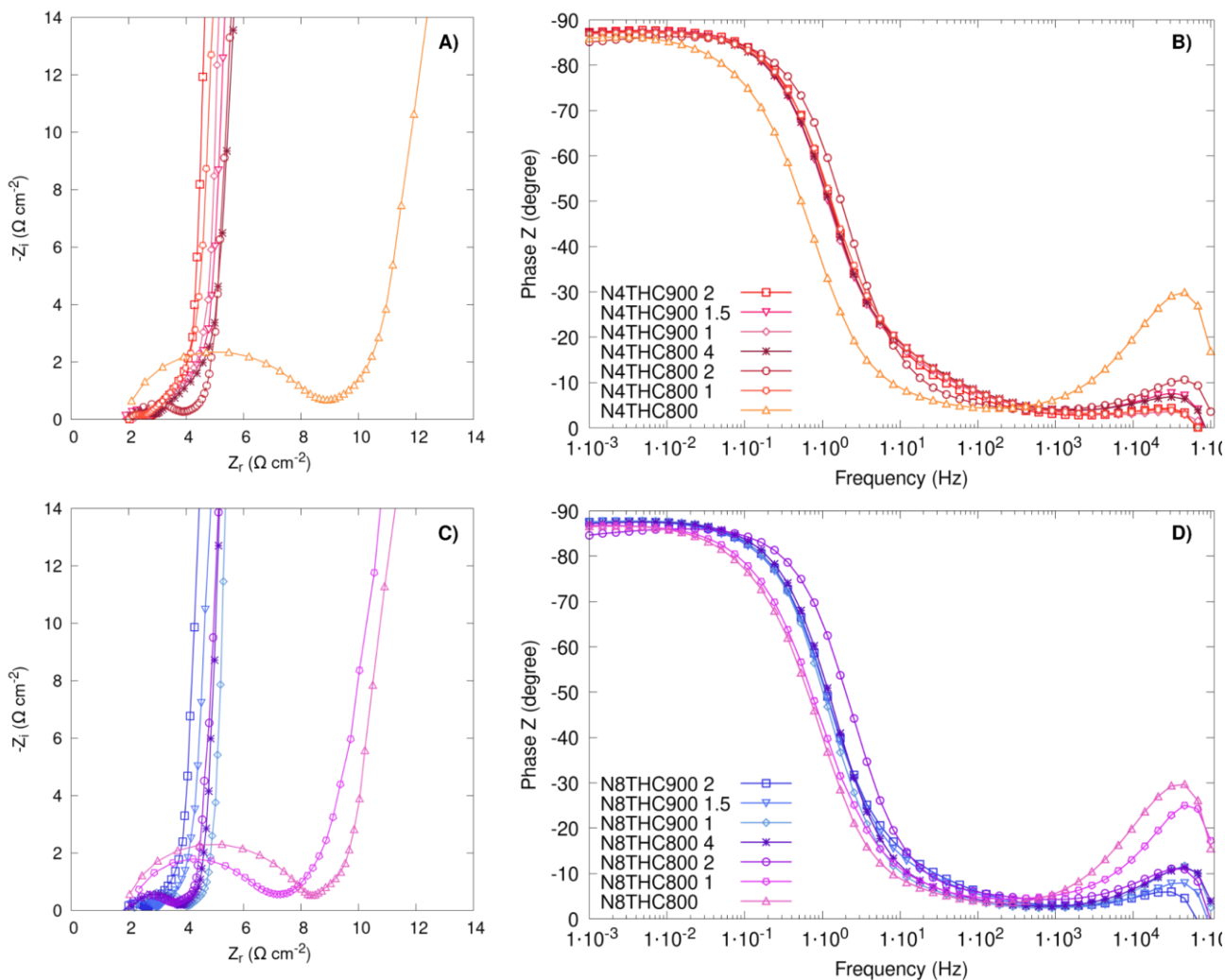


Figure S5 EIS results for N4THC series: A) Nyquist plot, B) Bode diagram; and N8THC series: C) Nyquist plot, and D) Bode diagram.

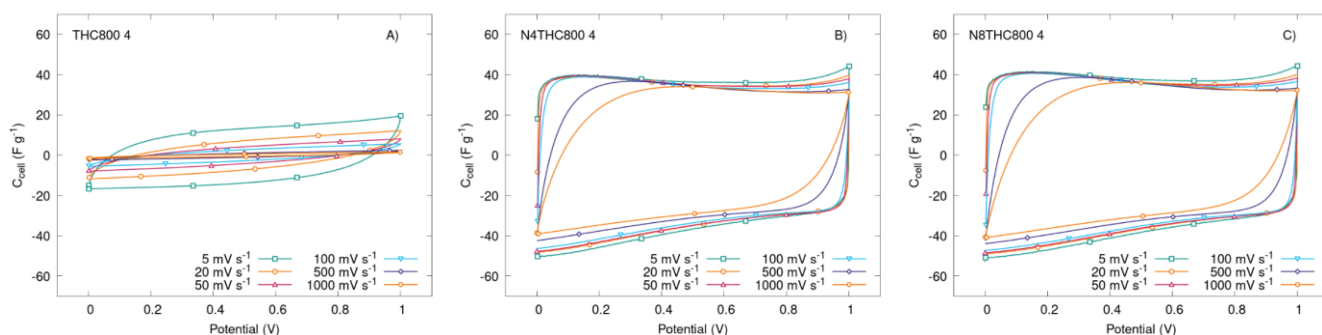


Figure S6. CV curves at different scan rates for the two-electrode system: A) THC800-4; B) N4THC800-4; and C) N8THC800-4 as electrode materials in 1 M H_2SO_4 .

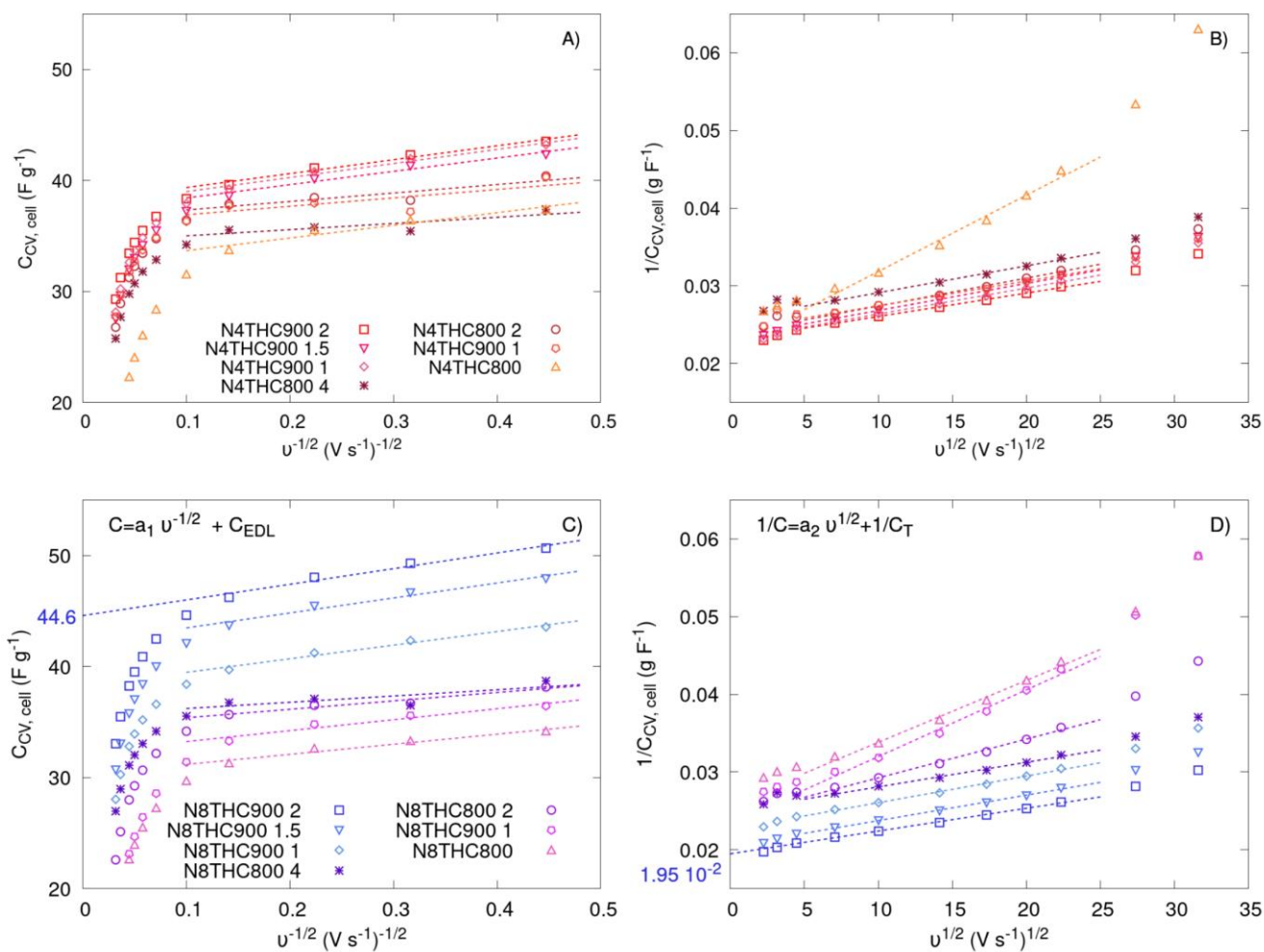


Figure S7. Dependence of capacitance on scan rate to differentiate pseudocapacitance (C_{PSC}) from double-layer capacitance (C_{EDL}) using Trassatti's method.

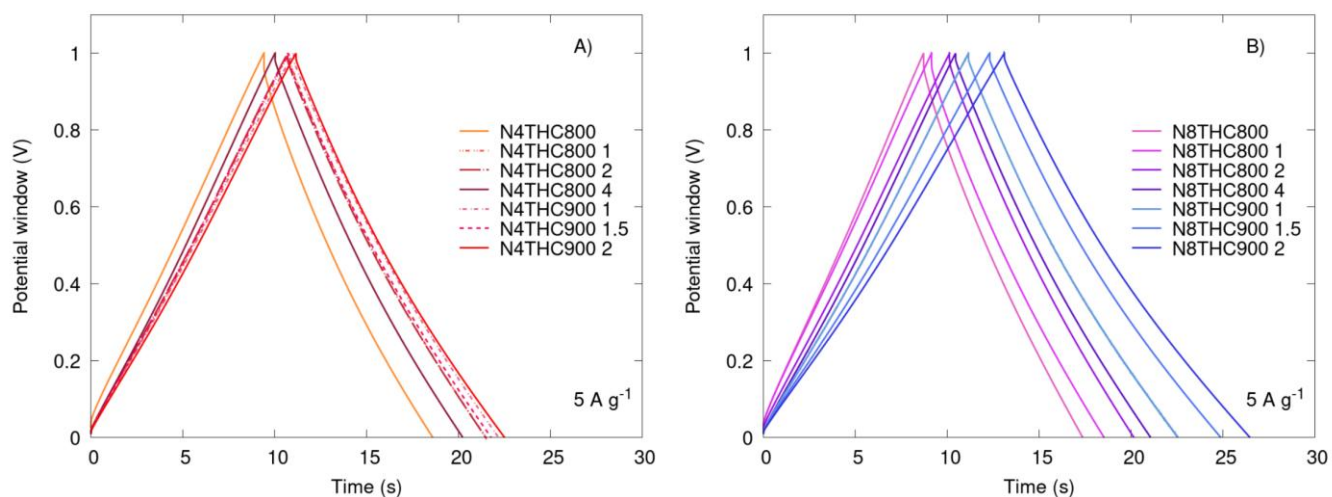


Figure S8. Galvanostatic charge-discharge curves at $5 A g^{-1}$: A) N4THC series; and B) N8THC series.